

# Characterization of precrystallization aggregation of canavalin by dynamic light scattering

Webe Kadima, Alexander McPherson, Michael F. Dunn, and Frances A. Jurnak

Department of Biochemistry, University of California at Riverside, Riverside, California 92521

**ABSTRACT** The aggregation processes leading to crystallization and precipitation of canavalin have been investigated by dynamic light scattering (DLS) in photon correlation spectroscopy (PCS) mode. The sizes of aggregates formed under various conditions of pH, salt concentration, and protein concentrations were deduced from the correlation functions generated by the fluctuating intensity of light scattered by the solutions of the protein. Results obtained indicate that the barrier to crystallization of canavalin is the formation of the trimer, a species that has been characterized by x-ray crystallographic studies (McPherson, A. 1980. *J. Biol. Chem.* 255:10472–10480). The dimensions of the trimer in solution are in good agreement with those obtained both from the crystal (McPherson, A.

1980. *J. Biol. Chem.* 255:10472–10480) and from a low angle x-ray scattering study in solution (Plietz, P., P. Damaschun, J. J. Müller, and B. Schlener. 1983. *FEBS [Fed. Eur. Biochem. Soc.] Lett.* 162:43–46). Furthermore, under conditions known to lead to the formation of rhombohedral crystals of canavalin, a limiting size is reached at high concentrations of canavalin. The size measured corresponds to an aggregate of trimers making a unit rhombohedral cell consistent with x-ray crystallographic data (McPherson, A. 1980. *J. Biol. Chem.* 255:10472–10480). Presumably, such aggregates are the nuclei from which crystal growth proceeds.

The present study was undertaken primarily to test the potential of DLS (PCS) as a tool for rapid, routine

screening to determine the ultimate fate of protein solutions (i.e., crystallization or amorphous precipitation) at an early stage, therefore eliminating the need for long-term visual observation. Achieving this goal would constitute a major advance in the practice of protein crystallization. Delays imposed by visual observation would be considerably reduced, and a more systematic approach could be adopted to select experimental conditions.

Our findings with canavalin demonstrate that DLS(PCS) is, indeed, a selective and sensitive probe of precrystallization conditions. Other advantages of this technique include the facts that it is noninvasive, nondestructive, universal, and does not require calibration.

## INTRODUCTION

The selection of optimal conditions for the crystallization of proteins has been and still remains a rather time-consuming process as the current state-of-the-art relies mostly on empirical rules and recipes. Despite the high potential for understanding functions through structure, very few, except for those with a long experience, would welcome, with enthusiasm, the task of crystallizing a protein.

"Trial and error . . . art rather than science . . . most protein crystals are still grown by brute force . . . procedures require investigations of large numbers of experimental conditions in hopes of finding the combination that produces usable crystals. . ." These are statements most often associated with protein crystallization (1). The present state of protein crystallization is a consequence of a lack of fundamental studies capable of providing guidelines for a systematic approach. Because crystallization is now the major obstacle to the determination of the three-dimensional structure of macromolecules, scientists

in this field are increasingly expressing the necessity for overcoming this impasse that has long plagued protein crystallization (1–4).

Despite the realization of the important need for fundamental studies on protein crystallization, experimental studies have been slow in coming. Approximately 10 years ago, for example, it was suggested that protein concentration dependence of the size distribution of small aggregates makes it possible to approach the problem of nucleation in a systematic way (5). The authors tested this hypothesis by applying the technique of quasielastic light scattering (QLS) using lysozyme as a model protein. Given the indicated potential of this technique, it is surprising that only a very limited interest has been shown in its use (6,7).

Since the appearance of the initial reports, the technique of QLS has evolved and benefited from technological advances and software implementations. Spectrum analyzers have been largely replaced by correlators.

Dynamic range problems, resulting from the coexistence of aggregates of significantly different sizes, have been overcome by the construction of multicorrelators.

Herein is reported a study of the precrystallization conditions of a major protein of the jack bean, canavalin, by dynamic light scattering (DLS) using photon correlation spectroscopy. This study demonstrates that measurement of aggregate sizes in the early stages of crystallization (prenucleation) carries information about the ultimate fate of the protein solution.

## MATERIALS AND METHODS

### Chemicals

Canavalin was isolated from jack bean meal according to a procedure previously described (8). The jack bean (*Canavalis ensiformis*) was obtained from Sigma Chemical Co., St. Louis, MO; sodium phosphate, ammonium hydroxide (NH<sub>4</sub>OH), and phosphoric acid (H<sub>3</sub>PO<sub>4</sub>) were obtained from Mallinckrodt Inc., St. Louis, MO; sodium chloride (NaCl) and potassium phosphate were obtained from Fisher Scientific Co., Pittsburgh, PA. All chemicals were used as obtained without further purification. Water was doubly distilled.

### Sample preparation

A concentrated solution of canavalin was prepared by dissolving canavalin in a minimum amount of buffer; undissolved material was taken into solution by adding a few drops of a 2 M NH<sub>4</sub>OH solution. This usually brought the solution to pH ~9. The resulting solution was centrifuged to clarify it of any remaining undissolved material. This stock solution was then dialyzed against a 50-mM, pH-7 phosphate buffer containing the desired concentration of NaCl. At high NaCl concentrations, the buffer was kept at a pH slightly higher than 7 to prevent precipitation during dialysis. The dialyzed solution was filtered twice through 0.2-μm filters. Dilute samples were prepared from the stock solution using appropriate amounts of stock and buffer that was also prefiltered. pH adjustments were made with 2 M solutions of NH<sub>4</sub>OH and H<sub>3</sub>PO<sub>4</sub>.

Dust was avoided as much as possible. Cleaned pipettes, vials, syringes, etc. were covered when stored. The interiors of vial caps were made of Teflon.

Crystallization conditions for canavalin are known from the literature (9). Rhombohedral crystals are formed when canavalin is incubated in 50 mM phosphate buffer, pH 7, containing 0.7% of NaCl. At 2% NaCl, canavalin does not crystallize but an amorphous precipitate is formed. At a higher concentration (4% NaCl), canavalin forms needlelike crystals. Therefore, to study the aggregation under crystallizing conditions or precipitating conditions, the concentration of NaCl was maintained at 0.7 or 2%, respectively.

### Measurements and instrumentation

Absorbance measurements were made on a model 8450 spectrophotometer (Hewlett-Packard Co., Palo Alto, CA). To determine the concentration of canavalin, solutions were diluted to yield absorbance measurements between 0.2 and 0.6. The concentration was calculated using  $E_{280}^{1\%} = 6.8$  (8, 10).

pH measurements were made on a PHM26 model pH meter. The meter was calibrated with Fisher buffers pH 4 and 7 or 7 and 10 at 22°C, depending on the pH region of interest.

Aged solutions were observed under a 10 × W.F. microscope (Bausch & Lomb Inc., Rochester, NY) to determine whether crystals or amorphous precipitates were formed.

Light scattering measurements were made in photon correlation mode. With this technique, the diffusion coefficient of the scatterer is calculated from the correlation function generated by the fluctuating intensity of the light scattered. Fluctuations in intensity are a result of Brownian motion of particles and this motion depends on particle size and shape as well as temperature and viscosity of the solution. The theory, techniques, and applications of photon correlation spectroscopy have been extensively reviewed in the literature (11–14), however, they will be briefly discussed here for the sake of completeness.

Correlation is a comparison process between two signals in time, i.e., it is a time domain function. It provides a measure of similarity. The correlation function between two signals  $V_1(t)$  and  $V_2(t)$  is mathematically expressed by

$$G_{12}(\tau) = \lim_{T \rightarrow \infty} \frac{1}{T} \int_{-T/2}^{+T/2} V_1(t) V_2(t + \tau) dt, \quad (1)$$

Where  $G_{12}(\tau)$  refers to the cross-correlation between two signals for a relative time offset of  $\tau$ . It is determined by multiplying one signal,  $V_1(t)$ , with the other signal shifted in time,  $V_2(t + \tau)$ , and then taking the integral of the product. Thus, correlation involves multiplication, time shifting (or delay), and integration.

The process of correlation between a signal and a delayed version of itself is known as autocorrelation, and may be expressed by:

$$G_{11}(\tau) = \frac{1}{T} \int_{-T/2}^{+T/2} V_1(t) V_1(t + \tau) dt. \quad (2)$$

In a digital system of signal processing, the time scale and amplitude functions are quantized. The integrals are changed into summations. Therefore the discrete autocorrelation function at delay time  $xT$  is defined as:

$$G(xT) = \frac{1}{N} \sum_{x=1}^N V(1) \cdot V(t + xT). \quad (3)$$

This is the type of correlation used herein to analyze the intensity fluctuations of light scattered.

Jakeman and Pike (15) have shown that the photon autocorrelation function from a system of monodisperse, compact particles is given by a single exponential decay:

$$C(\tau) = n^2 [1 + b \exp(-2\Gamma\tau)], \quad (4)$$

where  $\Gamma$  is the decay rate,  $n^2$  is proportional to the square of the total intensity, and  $b$  is an experimental constant. The decay rate is related to the diffusion coefficient of the scatterer through the equation

$$\Gamma = Dq^2, \quad (5)$$

where  $D$  is the diffusion coefficient and  $q$  is the scattering vector.  $q$  can be calculated from the equation

$$q = 4\pi \frac{n}{\lambda} \sin \frac{\sigma}{2}, \quad (6)$$

where  $\lambda$  is the wavelength,  $n$  the refractive index, and  $\sigma$  the scattering angle.

By fitting the measured function to a single exponential,  $D$  can be found. Having done this, the Stokes-Einstein equation can be used to

calculate the radius of the particles. The Stokes-Einstein equation is

$$D = \frac{kT}{6\pi\eta R_h}, \quad (7)$$

where  $k$  is the Boltzman constant,  $T$  is the temperature,  $\eta$  is the viscosity, and  $R_h$  is the hydrodynamic radius.

When there exists a distribution in size, the correlation function deviates from a pure exponential decay. For narrow spreads in size, the technique of cumulants analysis is applied to derive useful information about size and distribution width. In the cumulants analysis method, half the logarithm of the normalized correlation function is expressed as a power series expansion in  $\tau$  (16):

$$\frac{1}{2} \ln \left( \frac{G(\tau)}{G(\infty)} \right) = \sum_{j=1}^{\infty} (-1)^j \frac{k_j}{j} \tau^j. \quad (8)$$

The first and second cumulants are

$$k_1 = \bar{\Gamma} \quad (9)$$

$$k_2 = \bar{\Gamma}^2 - \bar{\Gamma}^2. \quad (10)$$

The mean translational diffusion is deduced from the first cumulant using the relation

$$\bar{D} = k_1/q^2. \quad (11)$$

$\bar{D}$  is then used to calculate the effective mean hydrodynamic radius  $\bar{R}_h$  through the Stokes-Einstein relation.

The width of the distribution is given by the magnitude of the second cumulant through the variance (10) and is referred to as the polydispersity

$$V: \frac{k_2^{1/2}}{k_1} = \frac{(\bar{\Gamma}^2 - \bar{\Gamma}^2)^{1/2}}{\bar{\Gamma}}. \quad (12)$$

Thus, the variance provides a measure of the width of the distribution of decay rates normalized by the mean.

Measurements were made on a Malvern 4700C submicro particle analyzer system (Malvern Instruments Inc., Southborough, MA). It was equipped with an eight-bit correlator capable of variable time expansion (VTE). Up to eight different sample times can be programmed for each measurement. This feature is required for handling samples of broad particle size distribution. The correlator uses cumulants analysis to deconvolute the correlation function. A 16-bit IBM-compatible processor with 256K memory handles all normal computing tasks.

The light source was a model 2020 argon laser (Spectra-Physics Inc., Mountain View, CA). The 488-Å line was employed in single line operation mode, with powers ranging from ~200 to 400 mW.

All sizes reported herein are the Z mean from the cumulants analysis.

## RESULTS

### Aggregation of canavalin in the presence of 0.7% wt/vol NaCl

Rhombohedral crystals are formed when canavalin is incubated in a 50-mM, pH-7 phosphate buffer containing 0.7% NaCl. Thus, the concentration of NaCl was fixed at 0.7% wt/vol and the effects of protein concentration and

pH on the average size of the aggregates were examined. Fig. 1 depicts the dependence of the average hydrodynamic diameter of the aggregates on the concentration of canavalin at pH 7 (curve *a*). Curve *b* is the change in polydispersity. Curve *a* can be divided into three distinct domains of concentrations and sizes. The first one (which is referred to as domain A) covers the range of concentrations 0.05–0.12%. It is a linear curve with a slope of 32 Å ml/mg. The average diameters measured in this domain range from 14 to 36 Å. The second domain (domain B) is characterized by a linear curve as well, but of higher slope (180 Å ml/mg). In this domain, sizes range from 44 to 214 Å reached at a concentration of 0.20% wt/vol of protein. Above this concentration, a distinctively different domain is formed that is mainly characterized by a high polydispersity. The measured average diameters range between 200 and 290 Å, and there is no clear trend to the change in diameter. The curve seems to have leveled off but with a large dispersion of the data points.

Solutions were allowed to equilibrate and were then observed under the microscope. All canavalin samples comprising domain A data remained clear (last observation made 104 d after preparation). Domain B samples became turbid and masses of deformed aggregates were observed under the microscope. Crystals were formed in domain C sample solutions by the third day after preparation. The behavior observed as the concentration of canavalin is increased indicates that the aggregates characteristic of the various concentration domains are of different nature and sizes. In domain A, the highest average diameter measured was 36 Å, which suggests that only the monomers exist in solution. Canavalin is a globular trimer with a diameter of 75 Å (Fig. 2 *a*) (17). The monomers of canavalin, as revealed by x-ray crystallographic studies, are of ellipsoidal form with minor and major axes of 35 and 50 Å, respectively (Fig. 2 *b*) (17). Using a modified Stokes-Einstein relation for a prolate

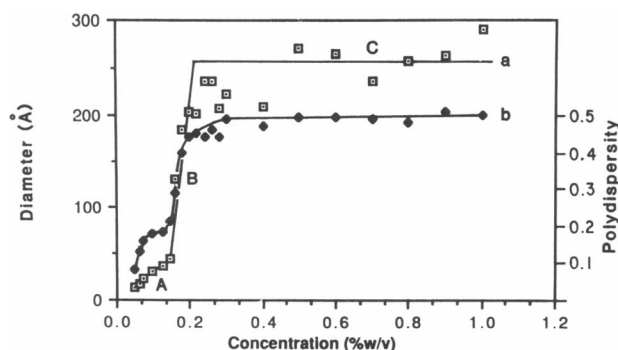


FIGURE 1 Concentration dependence of the measured, average hydrodynamic diameter (curve *a*) and the polydispersity (curve *b*) of canavalin species at pH 7 and 0.7% NaCl.

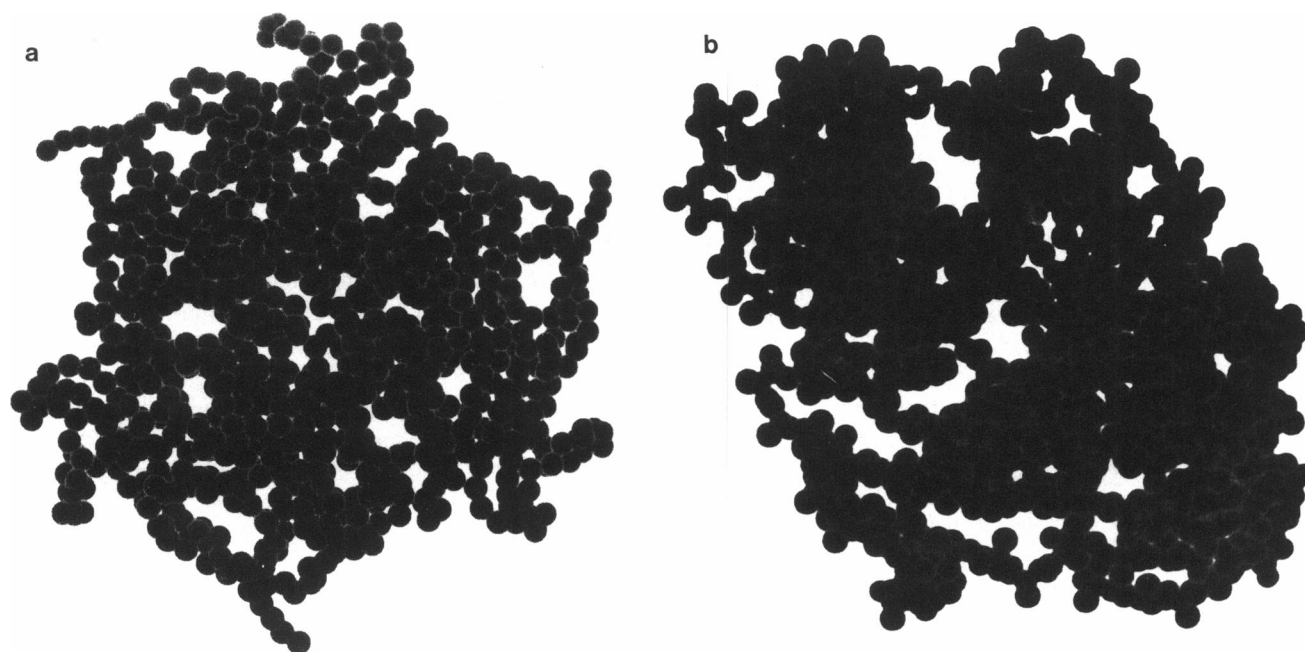


FIGURE 2 Computer-generated drawings of the trimer (a) and monomer (b) of canavalin.

ellipsoid (18) and the x-ray data for the monomer of canavalin, a diffusion coefficient of  $1.23 \cdot 10^{-6} \text{ cm}^2/\text{s}$  was calculated for our experimental conditions (temperature, 298 K; viscosity, 0.8905 Cp). According to the Stokes-Einstein relation, the equivalent spherical particle (i.e., of same diffusion coefficient), will have a hydrodynamic diameter of 40 Å under the same experimental conditions. Because the algorithm always assumes a spherical particle and utilizes the diffusion coefficient to calculate the hydrodynamic radius (or equivalent hydrodynamic radius in cases of nonspherical particles), 36 and 40 Å are, respectively, the experimental and calculated equivalent hydrodynamic diameters of the canavalin monomer. These values can be considered equal within the limits of experimental error. Furthermore, the Stokes-Einstein relation assumes that interactions between macromolecules have negligible effects both on the diffusion coefficients of individual aggregates and on the mean value of the diffusion coefficient. The effects of concentration on the diffusion coefficient are minimal if the macromolecules interact as hard spheres (19–23) and if the electrostatic interactions among particles are eliminated. The latter condition is fulfilled by adding neutral electrolyte to the system in a quantity sufficient to screen the electrostatic field ( $\sim 0.4 \text{ M}$ ) (19). The use of non-neutral electrolyte and the ellipsoidal shape of canavalin monomer are ample factors to account for the measured mean equivalent diameter of 36 Å for the canavalin monomer.

Also noteworthy in domain A is the change in polydis-

persity. It increases with concentration, then appears to plateau where monomers predominate in solution. A constant polydispersity, which marks the width of the distribution, indicates the existence of the same aggregate distribution, because our distribution was characterized by only two parameters, the mean and the variance.

As the second domain (B) begins to form, a sharp increase of the polydispersity simultaneously occurs. Once the measured average diameter exceeds 44 Å, a second but sharper increase in diameter of the aggregates is observed. In this region, the monomers are clearly forming a new type (or new types) of aggregates of increased size. The increased slope of the linear curve produced by data in this domain reflects stronger associative interactions between the aggregating entities. The upper region of this domain (concentration 0.3%) coincides with a measured mean diameter of 238 Å. It is interesting to note that this size approximates the expected diameter of an aggregate of eight canavalin trimers, placed at each lattice point of a rhombohedral cell as shown in Fig. 3 *a*. The maximum diameter joins opposite oligomers (Fig. 3 *b*) located along the threefold axis of symmetry. According to x-ray data (17) this diameter measures 234 Å, a value that compares well with the 238 Å measured by DLS(PCS) in the present study at 0.3% canavalin concentration. Crystals were formed in all samples of concentration higher than 0.3%. This observation suggests that formation of the aggregate previously described is essential for crystal growth to

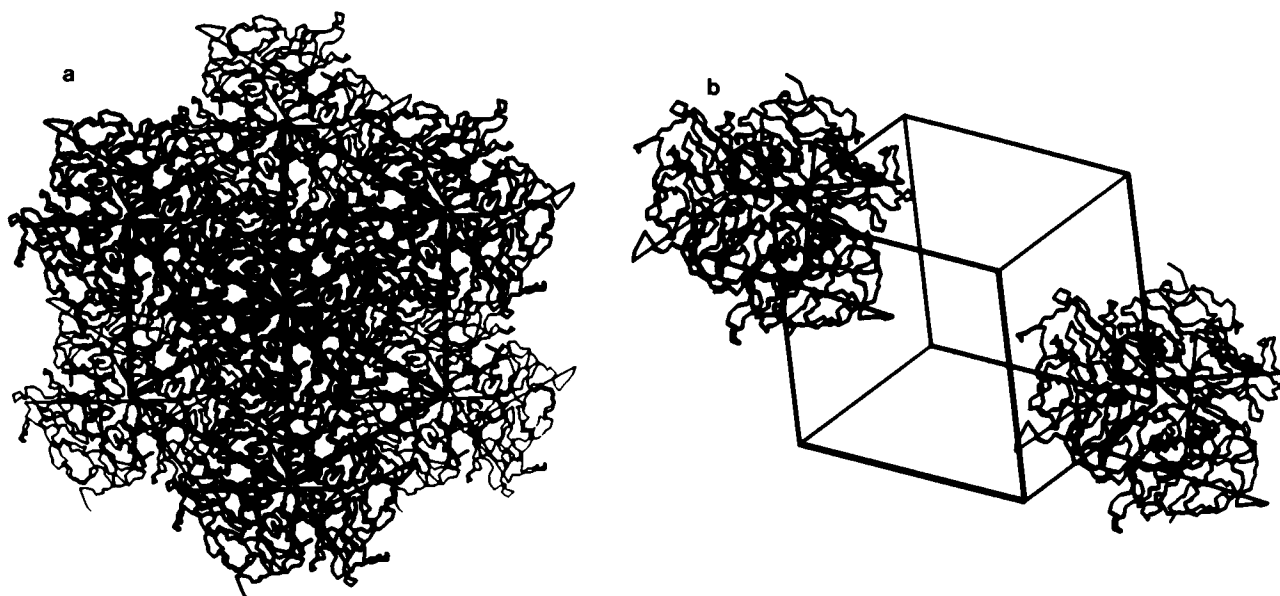


FIGURE 3 Computer-generated drawing of a canavalin aggregate formed at high concentrations of canavalin under conditions of pH 7 and 0.7% NaCl. (a) Rhombohedral unit cell fully occupied by eight canavalin trimers. (b) Rhombohedral unit cell with occupation of two opposite lattice points along the threefold axis of symmetry.

occur. It is, therefore, very likely that such aggregates are the nucleating centers in canavalin crystallization. Definition of the nuclei in a crystallizing system and knowledge of nuclei formation time and formation conditions could be very useful when attempting to grow large crystals. It is known that conditions which favor formation of nuclei result in an early cessation of growth (5). Thus, if alteration of conditions between nucleation and crystal growth can be achieved, both stages in crystallization would proceed optimally.

In domain C, the polydispersity is virtually constant and highest. Therefore, we conclude that there occurs a leveling effect on size in this domain, and the variation of observed mean diameter is a result of the large variance in the measurement. In fact, the average variance of 0.492 in this domain corresponds to a standard deviation of 7 Å which is comparable (within experimental error) to the deviation ( $\pm 18$  Å) from the mean of the values of diameters measured in domain C (255 Å).

The next step in our investigation was a study of the effect of pH on the nature of the canavalin aggregation processes. For this purpose, the concentration of canavalin was fixed at a level known to induce crystallization at pH 7. The average hydrodynamic diameter of the aggregate species in solution changes dramatically with the pH. Results obtained for solutions containing 0.5% wt/vol of canavalin are shown in Fig. 4. This curve of the dependence of hydrodynamic diameter on pH bears a striking resemblance to an acid-base titration curve with

an inflection point around pH 7.2. This similarity suggests a sharp and highly cooperative transition that modulates the nature of the species formed. Secondly, the occurrence of two limiting diameters at the low and high pH extremes indicates the existence of two species in the intermediate region.

Here again, the titration curve is characterized by domains which correspond to the different fates of canavalin in solution. Crystals formed in all samples of pH < 7 for which the average hydrodynamic diameters measured

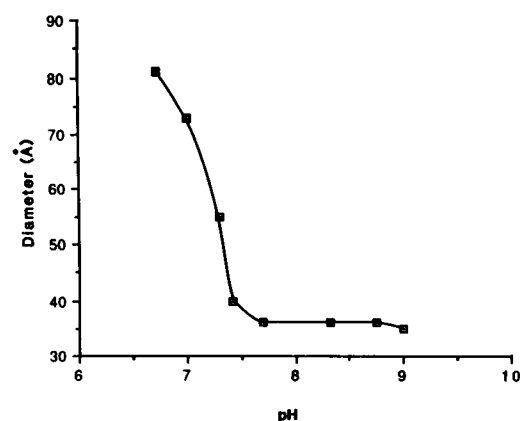


FIGURE 4 pH dependence of the measured average hydrodynamic diameter of canavalin species at 0.7% NaCl for a 0.5% wt/vol solution of canavalin.

were 73–81 Å. Amorphous aggregates were observed in all samples at pH >7.2. The mean hydrodynamic diameter obtained for the species in these solutions was 36 Å and constant for all the pH range >7.2. The numbers 81 and 36 Å correspond respectively to the hydrodynamic diameters of canavalin as a trimer and as a monomer. Thus, the behavior described above indicates that the barrier to crystallization of canavalin is set by the formation of the trimer, which depends on the concentration of canavalin, the pH of the solution and the concentration of NaCl. At high pH, the monomeric state predominates. The published procedure used to prepare single crystals of canavalin for x-ray analysis consists in slowly decreasing the pH of the solution from ~9 to pH 7 using the microevaporation technique (9). This method assures a slow induction of crystallization and growth which favors the formation of large crystals suitable for x-ray diffraction studies. Our results semiquantitatively affirm the validity of this approach. We speculate that when aggregation of monomers occurs too rapidly, formation of the trimers needed for crystallization does not occur. The clear discontinuity between the crystallization and precipitation regions demonstrates unambiguously the usefulness of such measurements in the selection of optimal conditions for the crystallization of proteins.

### Aggregation of canavalin in the presence of 2% NaCl

Canavalin does not crystallize when the concentration of NaCl is increased to 2%, rather deformed masses are observed under the microscope in mature solutions. The behavior of canavalin under these conditions was investigated to delineate differences in aggregation processes leading to crystallization from those leading to precipitation. Experiments similar to those of the preceding section were repeated but under conditions of 2% NaCl. Fig. 5 shows the dependence of the average hydrodynamic diameter on the concentration of canavalin at pH 7 and 2% NaCl. Similar to previous results, there is an increase in the size of the aggregate as the concentration is increased. However, the incremental increase in size with increasing concentration is much smaller. Furthermore, the curve defining this dependence is a monotonic linear progression, at least up to 0.8% wt/vol canavalin, with a much smaller slope compared to those of domains A and B in Fig. 1. The absence of any discontinuity in concentration dependence implies that the nature of the “interfaces” remain the same and aggregate growth is the only happenstance. The low slope is indicative of weaker interactions and is consistent with an earlier interpretation. The fact that this slope is less than that associated with the monomer, may be indicative of the formation of an entity different from the monomer. It is therefore,

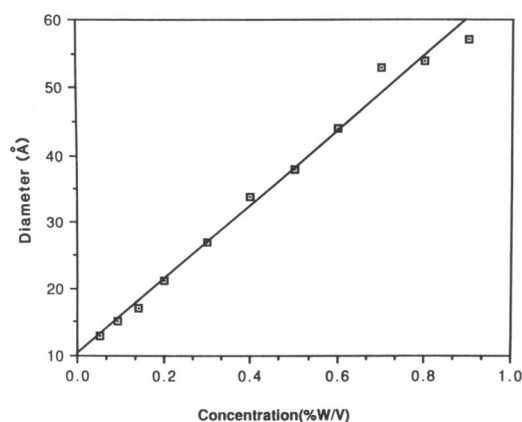


FIGURE 5 Concentration dependence of the measured average hydrodynamic diameter of canavalin species at pH 7 and 2% NaCl.

likely that the structure of aggregates which lead to amorphous precipitation have no resemblance to those which form crystals.

It has been suggested that amorphous precipitation can be approximated by a linear chain to which monomers can be added only at the ends (5). Thus, the incremental energy difference on adding a monomer is independent of the size of the aggregate. The results presented here support this assumption in that the incremental growth of the aggregate is constant throughout the range of concentrations examined. The formation of a crystal, however, is thought to proceed by addition of “monomers” in three dimensions. Before the aggregate reaches a critical size, from which point it grows spontaneously, it must overcome an energy barrier (5). Our results do not agree well with this pathway. Rather, for the canavalin system, formation of the trimer appears to be the limiting step in crystallization.

The effect of pH under conditions leading to amorphous precipitation further establishes that there is a substantial difference between processes leading to crystallization and to amorphous precipitation. The pH dependence at 2% NaCl is shown in Fig. 6 for 1% wt/vol solution of canavalin. Only a small increase in the hydrodynamic diameter is observed when the pH is lowered. Here again, no indication of monomer formation exists. The limiting average hydrodynamic diameter at the high pH is 13 Å, a value too small to represent any of the known species of canavalin (monomer or trimer). Note that this diameter is deduced from the Stokes-Einstein equation using the diffusion coefficient extracted from the correlation function. Therefore, a calculated small diameter may simply mean that the motional behavior of species existing in solution generates a correlation function with a short relaxation time. The measured diffusion coefficient calculated from the correlation function must

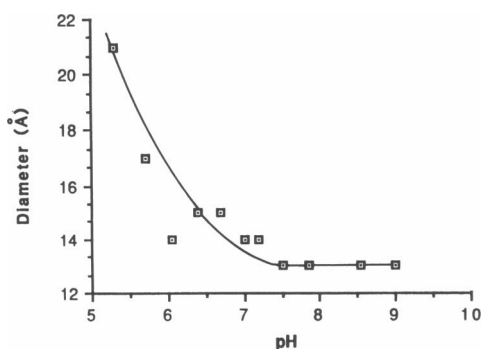


FIGURE 6 pH dependence of the measured average hydrodynamic diameter of canavalin species at 2% NaCl for a 1% wt/vol solution of canavalin.

be due either to the small size of particles or to high mobility (25). We speculate that the large diffusion coefficient found may be due here to the mobility of canavalin peptide chains in solution. The monomer of canavalin contains tightly associated peptide fragments of 24,000 and 12,000 plus 13,000 referred to as  $A_1$  and  $A_3 + A_4$ , respectively (8). This nomenclature is based on the fashion in which the canavalin precursor is proteolytically cleaved to crystallize canavalin (8). Results obtained here suggest that these peptide fragments are dissociated and are the aggregating entities under conditions which lead to precipitation of canavalin.

## CONCLUSIONS

The primary aim of this work is to explore the potential of DLS to differentiate between solutions that ultimately will crystallize from those that ultimately will form amorphous precipitate. This preliminary investigation on canavalin has, we believe, demonstrated the usefulness of DLS for that purpose. These results indicate that DLS studies such as those carried out for canavalin can define conditions which favor protein aggregation on a crystallization pathway. In the case of canavalin, we conclude that formation of the trimer is essential to crystallization. The concentration dependence of aggregate size revealed that much stronger associative interactions hold aggregating species in aggregates on their path to crystallization as compared to aggregates on their path to precipitation.

Extensive studies of the effects of salt concentration, temperature, and pH can be used to characterize the thermodynamics of the processes leading to crystallization (25–29). One must realize, of course, that the DLS results obtained depend on calculated distributions of species which may not correspond to the real sample distribution even when the average values are accurate.

However, in cases where the composition of the population distribution and the individual hydrodynamic diameters are known, a rigorous thermodynamic interpretation can be afforded. An example in the canavalin system is illustrated by the dependence of the measured hydrodynamic size on the pH. The observed behavior suggests that the sample consists of two species in the region of change, the one formed exclusively at the low pH with 81 Å average diameter and the other formed exclusively at the high pH with 36 Å average diameter. Work is in progress to characterize the thermodynamics of the aggregation of canavalin in solution by DLS. We are also investigating conditions under which canavalin crystallizes in other crystallographic unit cells. Canavalin has been successfully crystallized in several unit cells (17), having hexagonal, orthorhombic, rhombohedral, and cubic symmetry. Presumably the aggregates leading to the different crystal forms differ in size and shape and should be detected as such by DLS(PSC).

Light scattering measurements were conducted at the Chemistry Department of the California Institute of Technology. We would like to acknowledge technical support by Ray Goodrich and Tracey Handel. We thank Marie Greene for producing all the computer-generated drawings of canavalin used in this paper. We also thank Jane Horning for the isolation and purification of the canavalin from Jack Bean meal used in these studies.

This work was supported by a University of California Research and Training Biotechnology Program Fellowship to Webe Kadima.

Received for publication 29 December 1988 and in final form 24 July 1989.

## REFERENCES

1. Bugg, C. E. 1986. The future of protein crystal growth. *J. Cryst. Growth*. 76:535–544.
2. Durbin, S. D., and G. Feher. 1986. Crystal growth studies of lysozyme as a model for protein crystallization. *J. Cryst. Growth*. 76:583–592.
3. McPherson, A. 1985. Crystallization of macromolecules: general principles. *Methods Enzymol.* 114:112–127.
4. Rosenberger, F. 1986. Inorganic and protein crystal growth: similarities and differences. *J. Cryst. Growth*. 76:618–636.
5. Kam, F., H. B. Shore, and G. Feher. 1978. On the crystallization of proteins. *J. Mol. Biol.* 123:539–555.
6. Baldwin, E. T., D. V. Grumley, and C. W. Carter, Jr. 1986. Practical, rapid screening of protein crystallization by dynamic light scattering. *Biophys. J.* 49:17–48.
7. Carter, C. W., Jr., E. T. Baldwin, and L. Frick. 1988. Statistical design of experiment for protein crystal growth and use of precrystallization assay. *J. Cryst. Growth*. 90:60–73.
8. Smith, S. C., S. Johnson, J. Andrews, and A. McPherson. 1982. Biochemical characterization of canavalin, the major storage protein of jack bean. *Plant Physiol.* 70:1199–1209.
9. McPherson, A. 1982. Preparation and Analysis of Protein Crystals. John Wiley & Sons, Inc., New York. 371 pp.

10. Margalit, R., and E. Daniel. 1978. Subunit structure of canavalin. *Phytochemistry*. 17:1015-1016.
11. Chu, B. 1974. *Laser Light Scattering*. Academic Press, Inc., New York. 317 pp.
12. Berne, B. J., and R. Pecora. 1976. *Dynamic Light Scattering*. John Wiley & Sons, Inc., New York. 376 pp.
13. Dahneke, B. E. 1983. *Measurement of Suspended Particles by Quasi-Elastic Light Scattering*. John Wiley & Sons, Inc., New York. 569 pp.
14. Pecora, R. 1985. *Dynamic Light Scattering: Applications of Photon Correlation Spectroscopy*. Plenum Publishing Corp., New York. 420 pp.
15. Jakeman, F., and E. R. Pike 1968. The intensity-fluctuation distribution of Gaussian light. *J. Phys. A (Proc. Phys. Soc.)*. 1:128-138.
16. Koppel, D. E. 1972. Analysis of macromolecular polydispersity in intensity correlation spectroscopy: the method of cumulants. *J. Chem. Phys.* 57:4814-4820.
17. McPherson, A. 1980. The three-dimensional structure of canavalin at 3.0 Å resolution by x-ray diffraction analysis. *J. Biol. Chem.* 255:10472-10480.
18. Tanford, C. 1961. *Physical Chemistry of Macromolecules*. John Wiley & Sons, Inc., New York. 327 pp.
19. Pusey, P. N. 1974. Macromolecular diffusion. In *Photon Correlation and Light Beating Spectroscopy*. H. Z. Cummins and E. R. Pike, editors. Plenum Publishing Corp., New York.
20. Batchelor, G. K. 1974. Brownian diffusion of particles with hydrodynamic interaction. *J. Fluid Mech.* 74:1-29.
21. Pyun, C. W. 1964. Frictional coefficient of polymer molecules in solution. *J. Chem. Phys.* 41:937-944.
22. Phillies, G. D. J., G. B. Benedek, and N. A. Mazer. 1976. Diffusion in protein solutions at high concentrations: a study by quasielastic light scattering spectroscopy. *J. Chem. Phys.* 65:1883-1892.
23. Fair, B. D., and A. M. Jamieson. 1980. Effect of electrodynamic interactions on the translational diffusion of bovine serum albumin at finite concentration. *J. Colloid Interface Sci.* 73:130-135.
24. Schaefer, D. W. 1987. Quasielastic light scattering from dilute and semidilute polymer solutions. In *Dynamic Light Scattering: Applications of Photon Correlation Spectroscopy*. R. Pecora, editor. Plenum Publishing Corp., New York. 181-243.
25. Donovan, J. M., G. B. Benedek, and M. C. Carey. 1987. Self-association of human apolipoproteins A-I and A-II and interactions of apolipoprotein A-I with bile salts: quasi-elastic light scattering studies. *Biochemistry*. 26:8116-8125.
26. Donovan, J. M., G. B. Benedek, and M. C. Carey. 1987. Formation of mixed micelles and vesicles of human apolipoproteins A-I and A-II with synthetic and natural lecithins and the bile salt sodium taurocholate: quasi-elastic light scattering studies. *Biochemistry*. 26:8125-8133.
27. Mazer, N. A., M. C. Carey, R. F. Kwasnick, and G. B. Benedek. 1979. Quasielastic light scattering studies of aqueous biliary lipid systems. Size, shape, and thermodynamics of bile salt micelles. *Biochemistry*. 18:3065-3075.
28. Mazer, N. A., and M. C. Carey. 1983. Quasi-elastic light-scattering studies of aqueous biliary lipid systems. Cholesterol solubilization and precipitation in model bile solutions. *Biochemistry*. 22:426-442.
29. Missel, P. J., N. A. Mazer, G. B. Benedek, C. Y. Young, and M. C. Carey. 1980. Thermodynamic analysis of the growth of sodium dodecyl sulfate micelles. *J. Phys. Chem.* 84:1044-1057.